# ESTIMATION OF IRON-55 VOLUMETRIC CONTAMINATION VIA SURROGATES PRODUCED DURING Z-MACHINE OPERATIONS

A Thesis

by

JOHN FLORES-McLAUGHLIN

Submitted to the Office of Graduate Studies of
Texas A&M University
in partial fulfillment of the requirements for the degree of

MASTER OF SCIENCE

August 2008

Major Subject: Health Physics

# ESTIMATION OF IRON-55 VOLUMETRIC CONTAMINATION VIA SURROGATES PRODUCED DURING Z-MACHINE OPERATIONS

A Thesis

by

JOHN FLORES-McLAUGHLIN

Submitted to the Office of Graduate Studies of
Texas A&M University
in partial fulfillment of the requirements for the degree of

MASTER OF SCIENCE

Approved by:

| | |
|---|---|
| Chair of Committee, | Leslie A. Braby |
| Committee Members, | John Ford |
| | Michael Walker |
| Head of Department, | Raymond Juzaitis |

August 2008

Major Subject: Health Physics

# ABSTRACT

Estimation of Iron-55 Volumetric Contamination via Surrogates Produced During Z-Machine Operations. (August 2008)

John Flores-McLaughlin, B.S., Texas A&M University

Chair of Advisory Committee: Dr. Leslie A. Braby

Analysis of the radiation produced by Z-machine nuclear experiments at Sandia National Laboratory and the materials irradiated indicate that the majority of produced radionuclides can easily be detected. One significant exception is volumetric contamination of stainless steel by iron-55. Detecting iron-55 in Z-machine components presents a particular problem due to its low-abundance and the low-energy (5.9 keV) x-ray it emits. The nuclide is often below the minimum detectable activity (MDA) threshold and resolution criteria of many standard radiation detection devices. Liquid scintillation has proven useful in determining iron-55 presence in loose contamination at concentrations below that of regulatory guidelines, but determination of volumetric iron-55 contamination remains a significant challenge. Due to this difficulty, an alternate method of detection is needed. The use of radioactive surrogates correlating to iron-55 production is proposed in order to establish an estimate of iron-55 abundance.

The primary interaction pathways and interaction probabilities for all likely radionuclide production in the Z-machine were tabulated and radionuclides with production pathways matching those of iron-55 production were noted. For purposes of

nuclide identification and adequate detection, abundant gamma emitters with half-lives on the order of days were selected for use as surrogates.

Interaction probabilities were compared between that of iron-55 production and a chosen surrogate. Weighting factors were developed to account for the differences in the interaction probabilities over the range of the known energy spectra produced on the device.

The selection process resulted in cobalt-55, cobalt-57 and chromium-51 as optimal surrogates for iron-55 detection in both deuterium and non-deuterium loaded interactions. A decay corrected correlation of the surrogates (chromium-51, cobalt-57 and cobalt-55) to iron-55 for deuterium and non-deuterium loaded Z-machine driven reactions was derived.

The weighting factors presented here are estimates which are based on rough comparisons of cross-section graphs. Analysis considering factors such as energy spectrum criteria to provide refined weighting factors may be utilized in future work.

# ACKNOWLEDGEMENTS

I would like to thank my committee chair, Dr. Braby and my committee members, Dr. Ford, and Dr. Walker for their guidance and support throughout my coursework and this research. I would also like to thank Dr. John Poston for his guidance editing this thesis and my fellow peers for their support.

This research was made possible due to the support and use of facilities of the Sandia National Laboratory radiation protection organization. I would like to thank Bradley Elkin, Todd Culp, Robert Miltenberger, Tony Brock and the rest of the division for the support with data collection and analysis for this paper.

I also want to extend my gratitude to the National Science Foundation Bridge to the Doctorate program which provided the primary funding and scholarly discussions towards this academic pursuit.

# NOMENCLATURE

| | |
|---|---|
| MDA | Minimum Detectable Activity |
| Fe | Iron |
| Cr | Chromium |
| Co | Cobalt |

TABLE OF CONTENTS

# LIST OF FIGURES

# LIST OF TABLES

# 1. INTRODUCTION

The Sandia National Laboratory Z-machine located in Albuquerque, NM is a large x-ray and magnetic field generator designed to test materials in extreme temperature and pressure. The Z-machine fires a very powerful electrical discharge ($10^7$ ampere for less than 100 nanoseconds) into an array of thin, parallel tungsten wires. The high electrical current vaporizes the wires which are transformed into highly ionized plasma. Simultaneously, the current density induces a powerful magnetic field which radially compresses the plasma into a cylindrical orientation. The vertical cylinder's axis is conventionally termed the z-axis, hence the name "Z-machine". The imploding plasma produces high temperature, x-ray pulse and can cause a shockwave. In some experiments the gas surrounding the wires is replaced by deuterium in order to provide additional desired interactions, primarily fusion which was first observed in 2003. During this intense release of energy and simultaneous ionization, several nuclear interactions take place producing assorted radionuclides.

The concentration of these radionuclides in Z-machine components is a key item of interest in regulatory limits and procedures. A number of these radionuclides are produced at levels that may not provide for deterministic health risk, but remain a regulatory concern.

Of these radionuclides, iron-55 is of particular concern because current detection and mitigation methods are unlikely to detect it. The levels present are likely lower than the

---

This thesis follows the style of Radiation Measurements.

minimum detectable activity (MDA). The primary low energy x-rays produced in iron-55 are often indistinguishable when observed in multiple radionuclide spectroscopy. Liquid scintillation detection has proven useful in detecting iron-55 in loose contamination and results in MDA lower than regulatory thresholds, but a direct method to measure volumetric contamination has not been established.

The material of interest is 304 stainless steel since it is the only material on the Z-machine with significant concentrations of elements that can be converted to iron-55 as established by previous interaction studies (Culp, 2007). A list of most prevalent primary Z-machine interactions and their respective radionuclide products in 304 stainless steel are provided in Tables A, B, C and D of the Appendix.

Detected levels of several of these radionuclides strongly indicate iron-55 production mechanisms occurring during Z-machine reactions. These radionuclides prove useful as surrogates indicating the presence of iron-55 and are the basis of the proposed detection method.

Five interaction mechanisms in 304 stainless steel are significant for iron-55 production. Other interaction mechanisms exist but will result in much lower levels of iron-55 and are deemed negligible. Iron-55 is produced directly through (d, p), (n, $\gamma$) and (p, n) projectile-ejection interactions in 304 stainless steel. It is also noted that cobalt-55 decays to iron-55, so all cobalt-55 detected contributes to iron-55 abundance. The primary production mechanisms of iron-55 are shown below in Tables 1 and 2.

Table 1. Direct production of Iron-55. National Nuclear Data Center. Nuclear Science References, (2007). Information extracted from the NSR database.

| Target | Reaction | Target Abundance (%) | Produced Radionuclide | Half Life | Q (MeV) |
|---|---|---|---|---|---|
| Fe-54 | d, p | 4 ± 0 | Fe-55 | 2.7y | 7.58 |
| Fe-54 | n, γ | 4 ± 0 | Fe-55 | 2.7y | 9.3 |
| Mn-55 | p, n | < 2 | Fe-55 | 2.7y | -1.52 |

Table 2. Indirect production of Iron-55. National Nuclear Data Center. Nuclear Science References, (2007). Information extracted from the NSR database.

| Target | Reaction | Target Abundance (%) | Produced Radionuclide | Half Life | Q (MeV) |
|---|---|---|---|---|---|
| Fe-54 | p, γ | 4 ± 0 | Co-55 | 17.5 h | 5.06 |
| Fe-54 | d, n | 4 ± 0 | Co-55 | 17.5 h | 2.83 |

Accounting for each of the interaction pathways by radioactive surrogates will serve as a useful method of estimating iron-55 abundance.

# 2. METHOD

The primary interaction pathways for expected radionuclide production in the Z-machine are tabulated in Tables A, B, C and D of the Appendix. Several radionuclides with production pathways matching those of iron-55 production can be observed. A process of elimination was pursued to identify radionuclides for possible use as a surrogate for iron-55 detection. The chosen surrogates must both have a reasonable half-life and emit radiation that is easy to detect.

For purposes of nuclide identification and adequate detection, radionuclides with abundant gamma emissions and half-lives on the order of days will be selected for use as surrogates. Gamma emission is necessary for accurate radionuclide identification. Detection usually takes place within days after a Z-machine session. Surrogates with half-lives on the order of days were chosen to ensure adequate activity above the MDA when measurements are made. Due to the additional presence of deuterium in some experiments, the method of surrogate detection must be differentiated for deuterium and non-deuterium loaded shots. The presence of deuterium causes several additional interactions with additional production pathways for iron-55 that must be accounted for. A proton flux component is present and contributes to interactions taking place in both deuterium and non-deuterium loaded interactions.

Each production pathway results in a number of different potential surrogates. By relating the surrogate activity back to that of iron-55, an estimate of iron-55 may be established. Relating surrogate activity to iron-55 requires the use of some weighting factors to account for differences in their respective production mechanisms. Weighting

factors relating the atomic abundances of the target materials, interaction probability and corrections for decay time differences are implemented in the final mathematical expressions.

To account for the difference in target abundance between that of a produced surrogate and iron-55, a weighting factor correlating the initial isotopic abundances of the target nuclei will be implemented in the final mathematical correlation. To account for difference in relative interaction probabilities a ratio of interaction probabilities will be determined as follows over a set energy range E1 to E2:

$$F = \frac{\int_{E1}^{E2} \sigma_2(E)dE}{\int_{E1}^{E2} \sigma_1(E)dE} \qquad (1)$$

Where F is given as the interaction probability weighting factor used to relate a production surrogate to iron-55 production. These factors are expected to be modified as data is obtained and updated.

# 3. IRON-55 IN DEUTERIUM LOADED REACTIONS

Each production pathway can be accounted for by a number of different surrogates. By relating the surrogate activity back to that of iron-55, an estimate of iron-55 may be established. A process of elimination was pursued among the radionuclides present. A compiled list of expected radionuclides in deuterium-loaded interactions from 304 stainless steel can be found on Table 3.

Table 3. Radionuclides from deuterium loaded interactions. National Nuclear Data Center. Nuclear Science References, (2007). Information extracted from the NSR database.

| **Target: 304 Stainless steel** Detected nuclide | Half-life | Production reaction | Daughter | Daughter Half-life |
|---|---|---|---|---|
| Co-54 | 1.5m/193ms | p, n | Fe-54 | Stable |
| **Co-55** | **17.5 h** | **p, γ; d, n** | **Fe-55** | **2.73 yr** |
| Co-56 | 77.3d | p, n | Fe-56 | Stable |
| **Co-57** | **271d** | **d, n; p, n** | **Fe-57** | **Stable** |
| Co-58 | 9.1h/71d | d, n | Fe-58 | Stable |
| Mn-50 | 1.7m/283ms | p, n | Cr-50 | 1.8E+17 yr |
| Mn-51 | 46.2m | d, n | Cr-51 | 27d |
| Mn-52 | 21m/5.6d | p, n | Cr-52 | Stable |
| Mn-53 | 3.7x106y | p, n; d, n | Cr-53 | Stable |
| Mn-54 | 312 d | p, n; d, n | Cr-54 | Stable |
| Mn-56 | 2.6h | d, p; n, γ | Fe-56 | Stable |
| Cu-58 | 3.2s | p, n | Ni-58 | Stable |
| Cu-59 | 1.4m | d, n | Ni-59 | 7.6E+4 yr |
| Cu-60 | 24ms | p, n | Ni-60 | Stable |
| Cu-61 | 3.4h | p, n; d, n | Ni-61 | Stable |
| Cu-62 | 9.7m | p, n; d, n | Ni-62 | Stable |
| Fe-55 | 2.73 y | p, n; d, p; n, γ | Mn-55 | Stable |
| **Cr-51** | **27d** | **d, p; n, γ** | **V-51** | **Stable** |
| Cr-55 | 3.5m | d, p; n, γ | Mn-55 | Stable |
| Ni-59 | 7.6x104y | d, p; n, γ | Co-59 | Stable |
| Ni-63 | 101y | d, p; n, γ | Cu-63 | Stable |

As can be observed in Table 3, several production pathways exist with interaction probabilities comparable to iron-55. Applying radiation type and half-life selection criteria of abundant gamma-emitters with half-lives on the order of days eliminates the majority for possible use as a surrogate. The surrogates best suited for this purpose have been determined as chromium-51, cobalt-55 and cobalt-57 from Table 3. Weighting factors relating the atomic abundances of the target materials, interaction probability and correcting for decay time discrepancy are implemented in the final mathematical expressions as described in the following sections.

## 3.1 Cobalt-55 Decay

Cobalt-55 decays directly to iron-55 with a 17.5 hour half life. Therefore all cobalt-55 detected must contribute to iron-55 abundance. A decay corrected expression is presented to correlate cobalt-55 that has decayed to iron-55. The decay-corrected abundance of iron-55 from cobalt-55 decay as a function of time is given by Equation 2.

$$N(t)^{Co55\rightarrow}_{Fe-55} = [N(t)^{Fe55}] * e^{(-\lambda_{Fe55}t)}$$

$$N(t)^{Co55\rightarrow}_{Fe-55} = [A^{total}_{0\,Co-55}\int_0^t e^{(-\lambda_{Co55}t)}dt] * e^{(-\lambda_{Fe55}t)}$$

$$A(t)^{Co55\rightarrow}_{Fe-55} = N(t)^{Co55\rightarrow}_{Fe-55} * \lambda_{Fe55}$$

$$A(t)^{Co55\rightarrow}_{Fe-55} = [\frac{A^{total}_{0\,Co-55}}{\lambda_{Co55}}(1-e^{(-\lambda_{Co55}t)})] * e^{(-\lambda_{Fe55}t)} * \lambda_{Fe55} \qquad (2)$$

Where $A(t)^{Co55\rightarrow}_{Fe-55}$ is activity of the iron-55 from cobalt-55 decay as a function of time, $A^{total}_{0\,Co-55}$ is the initial activity of cobalt-55 and $\lambda_{Co55}$ is the decay constant for cobalt-55.

## 3.2 Chromium-51 by (d, p) and (n, γ) Interaction

Chromium-51 has been detected in previous Z-machine experiment sessions. Interestingly, the Fe-54 (d, p) Fe-55 and Fe-54 (n, γ) Fe-55 direct production reactions have similar production rates to Cr-50 (d, p) Cr-51 and Cr-50 (n, γ) Cr-51. In addition, chromium-51 is only produced directly by these reactions (indirectly by manganese-51 decay). A correction factor will be developed to account for subsequent manganese-51 decay. A relative comparison of each production method is shown below in Table 4.

Table 4. Cr-51 and Fe-55 by (d, p) and (n, γ) interactions. National Nuclear Data Center. Nuclear Science References, (2007). Information extracted from the NSR database.

| Target | Reaction | Target Abundance (%) | Produced Radionuclide | Half-Life | Q (MeV) |
|---|---|---|---|---|---|
| Fe-54 | d, p | 4 ± 0 | Fe-55 | 2.7y | **7.58** |
| Cr-50 | d, p | 0.8 ± 0.09 | Cr-51 | 27d | **7.56** |
| Fe-54 | n, γ | 4 ± 0 | Fe-55 | 2.7y | **9.3** |
| Cr-50 | n, γ | 0.8 ± 0.09 | Cr-51 | 27d | **9.27** |

The respective Q-values of interaction for each production mechanism are almost identical, contributing to similarity between the interactions. In addition, reaction threshold energy contribution due the coulomb barrier is relatively equal due to the similar charge of both target nuclides. Interaction probability data shows (n, γ) interactions between iron-54 and chromium-50 are within an order of magnitude of each other as shown below in Figure 1.

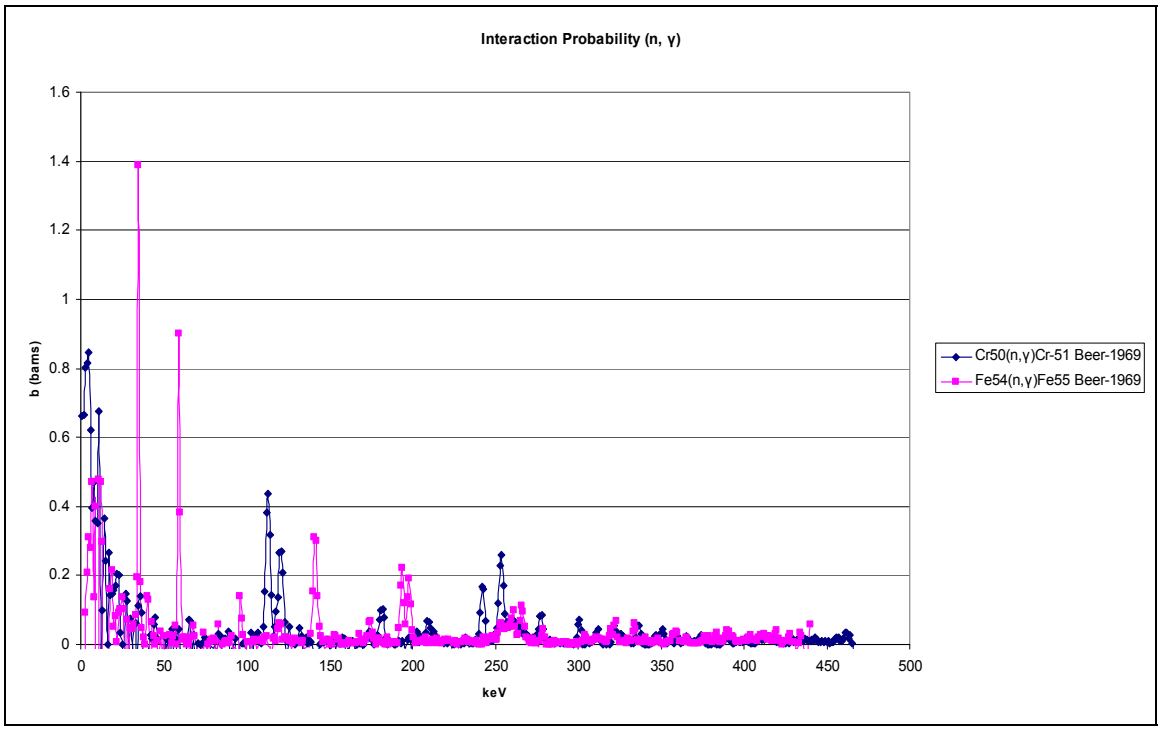


Fig. 1. Cr-50 (n, γ) Cr-51 and Fe-54 (n, γ) Fe-55 probability vs. incident neutron energy. Plot produced using the code JANIS, written by the OECD Nuclear Energy Agency and Aquitaine Electronique Informatique. OECD Nuclear Energy Agency. Le Seine Saint-Germain, France.

With this almost identical production probability of chromium-51 and iron-55 from (n, γ) interaction, one can estimate that chromium-51 production from (n, γ) interaction will be relatively equal to that of iron-55 from (n, γ) interaction.

Interaction probability data for Fe-54 (d, p) Fe-55 is very limited, but what has been obtained is within an order of magnitude to that of Cr-50 (d, p) Cr-51 interaction probability. The probabilities are shown in Figure 2.

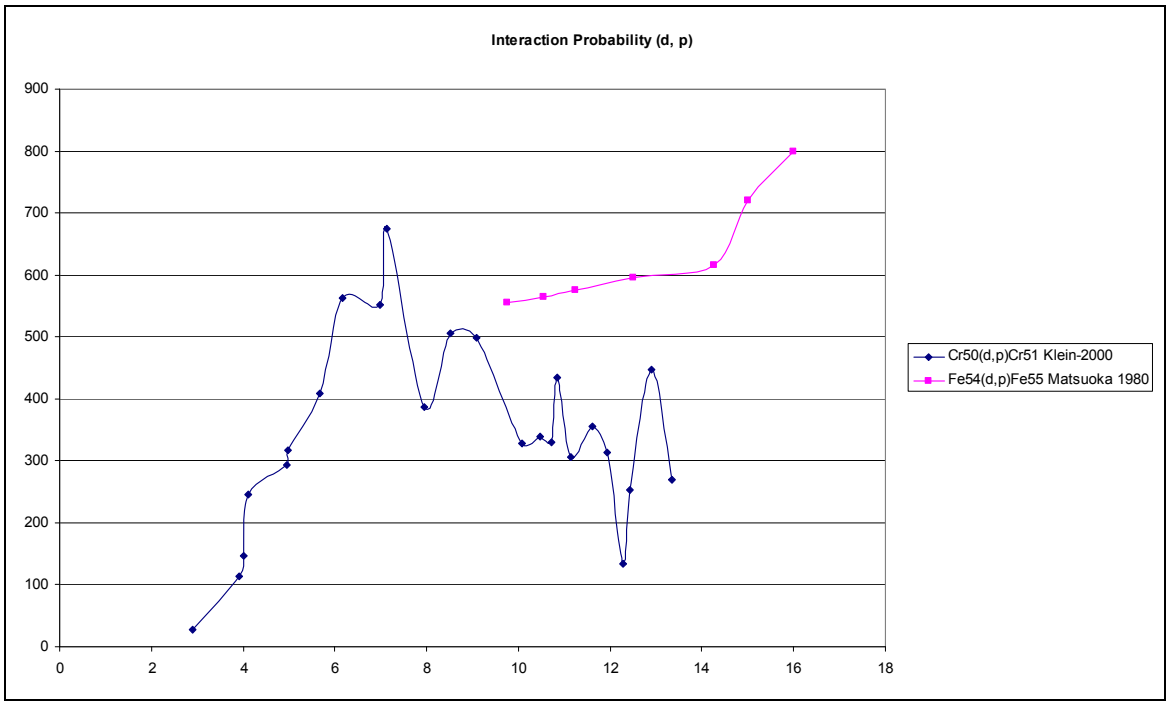


Fig. 2. Cr-50 (d, p) Cr-51 and Fe-54 (d, p) Fe-55 probability vs. incident deuteron energy. Plot produced using the code JANIS, written by the OECD Nuclear Energy Agency and Aquitaine Electronique Informatique. OECD Nuclear Energy Agency. Le Seine Saint-Germain, France.

To ratio the production of iron-55 to that of chromium-51 per atom a weighting factor of interaction probabilities from above is applied. The weighting factor can be applied to a specific energy range if applicable. If additional data is gathered for these (d, p) interactions the weighting factor may be updated to weight interaction probabilities properly. This interaction probability weighting factor will be notated $F_{(d,\ p;\ n,\ \gamma)}^{Fe55}{}_{Cr51}$ and will represent relative interaction probability.

With both probabilities of interaction within order of magnitude from what is shown, iron-55 production from both (n, gamma) and (d, p) interaction can reasonably be estimated from chromium-51 detection.

To account for chromium-51 contribution from manganese-51 decay, the activity of manganese-51 must be established. However, due to its extremely short half-life manganese-51 is difficult to detect. A surrogate must be established to account for

manganese-51 activity. Cobalt-55 is selected due to its similar production characteristics. This will be explained in the correction factor subsection.

*Chromium-51 Correction Factor*

As discussed previously, production of manganese-51 must be established to account for additional production (via decay) to chromium-51. Manganese-51 is produced by (d, n) interactions and hard to detect due to its short half-life. Cobalt-55 is already accounted for in this method and has near identical production interaction by (d, n) to manganese-51.

Cobalt-55 is rarely seen in non-deuterium reactions, unless the experimental setup changes significantly to allow for relatively higher (at least three orders of magnitude higher) proton flux, the (p, γ) interaction pathway for cobalt-55 is negligible. The probability of interaction for this proton absorption process is three orders of magnitude lower than competing processes. Due to this negligible production mechanism, cobalt-55 can be used as a surrogate for manganese-51. The production characteristics of cobalt-55 and manganese-51 are shown in Table 5.

Table 5. Co-55 and Mn-51 by (d, n) interaction. National Nuclear Data Center. Nuclear Science References, (2007). Information extracted from the NSR database.

| Target | Reaction | Target Abundance (%) | Produced Radionuclide | Half Life | Q (MeV) |
|---|---|---|---|---|---|
| Fe-54 | d, n | 4 ± 0 | Co-55 | 17.5 hr | **2.83** |
| Cr-50 | d, n | .8 ± .09 | Mn-51 | 46.2 m | **3.08** |

Within an order of magnitude interaction probabilities of Fe-54 (d, n) Co-55 and Cr-50 (d, n) Mn-51 are shown in Figure 3.

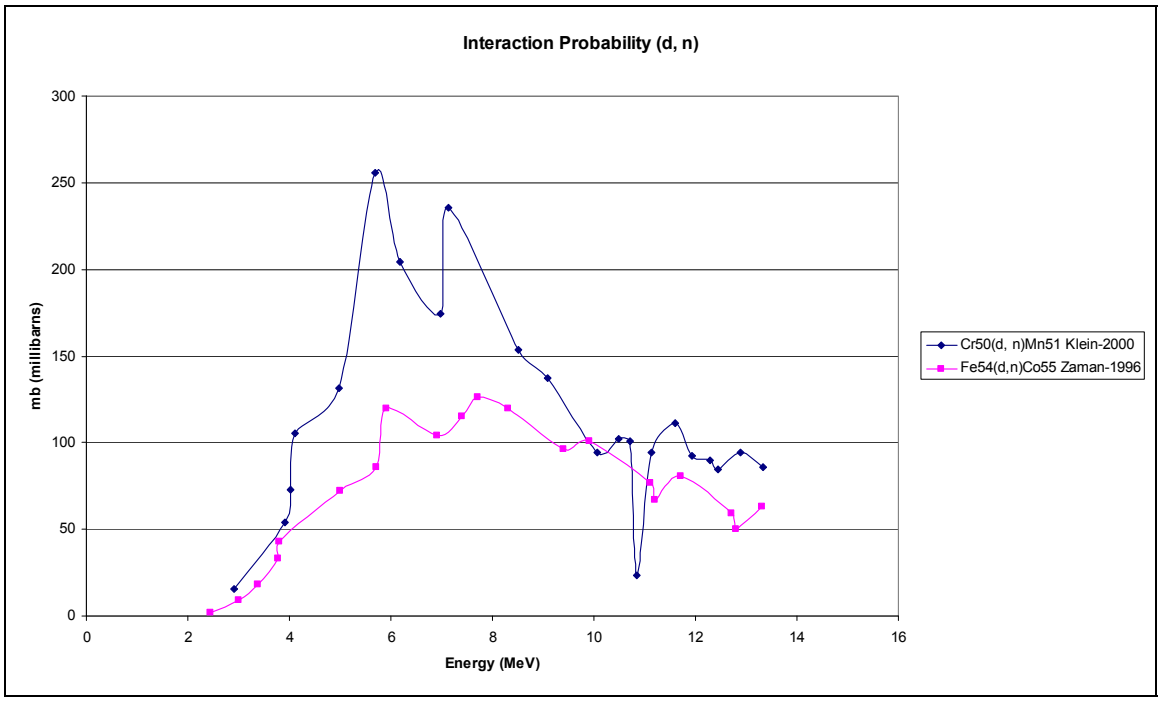


Fig. 3. Fe-54 (d, n) Co-55 and Cr-50 (d, n) Mn-51 probability vs. incident deuteron energy. Plot produced using the code JANIS, written by the OECD Nuclear Energy Agency and Aquitaine Electronique Informatique. OECD Nuclear Energy Agency. Le Seine Saint-Germain, France.

Due to the relative production probability of cobalt-55 to manganese-51, cobalt-55 can be used to estimate manganese-51, and therefore estimate how much chromium-51 was produced as a result of manganese-51 decay. A respective interaction probability weighting factor $\boldsymbol{F(d,n)^{Mn51}_{Co55}}$ can be established from the relative interaction probabilities.

*Chromium-51 Mathematical Correlation*

As previously described cobalt-55 can represent manganese-51 production, due to nearly identical interaction probability. The following is the decay corrected chromium-51 activity of (d, p) and (n, γ) interaction.

$$A_{0_{Cr-51}}^{d,p;n,\gamma} = A_{0_{Cr-51}}^{total} - A_{0}^{Mn-51}$$

$$\frac{A_{0}^{Mn-51}}{A_{0_{Co-55}}^{total}} = \frac{.008 \pm 0.0009}{.04} * F(d,n)_{Co55}^{Mn51}$$

Where .008/.04 is the ratio of the iron-54 and chromium-51 target abundances found in 304 stainless steel. $A_0$ is the activity of the respective radionuclide at time = 0 and $\boldsymbol{F(d,n)_{Co55}^{Mn51}}$ is equal to the interaction probability weighting factor as described.

$$A_{0_{Cr-51}}^{d,p;n,\gamma} = A_{0_{Cr-51}}^{total} - \frac{.008 \pm 0.0009}{.04} * A_{0_{Co-55}}^{total} * F(d,n)_{Co55}^{Mn51}$$

The $A_{0_{Cr-51}}^{d,p;n,\gamma}$ activity is representative of chromium-51 produced by (d, p) and (n, gamma) reactions. This is comparable to iron-55 production by (d, p) and (n, γ) interaction. The decay corrected activity of iron-55 from these mechanisms is shown below.

$$\frac{A_{0\,Fe-55}^{d,p;n,\gamma}}{A_{0\,Cr-51}^{d,p;n,\gamma}} = \frac{.04}{.008\pm0.0009} * F_{(d,\,p;\,n,\,\gamma)\,Cr51}^{Fe55}$$

$$A_{0\,Fe-55}^{d,p;n,\gamma} = \frac{.04}{.008\pm0.0009} * A_{0\,Cr-51}^{d,p;n,\gamma} * F_{(d,\,p;\,n,\,\gamma)\,Cr51}^{Fe55}$$

Where .04/.008 is the ratio of the iron-54 to chromium-54 target abundances found in 304 stainless steel. The decay corrected correlation to iron-55 by chromium-51 is derived in Equation 3.

$$A(t)_{Fe-55}^{d,p;n,\gamma} = A_{0\,Fe-55}^{d,p;n,\gamma} * e^{(-\lambda_{Fe55}t)}$$

$$A(t)_{Fe-55}^{d,p;n,\gamma} = \frac{.04}{.008\pm0.0009} * F_{(d,\,p;\,n,\,\gamma)\,Cr51}^{Fe55} * A_{0\,Cr-51}^{d,p;n,\gamma} * e^{(-\lambda_{Fe55}t)} \qquad (3)$$

Where $\boldsymbol{F_{(d,\,p;\,n,\,\gamma)\,Cr51}^{Fe55}}$ is equal to the respective interaction probability weighting factor.

### 3.3 Cobalt-57 by (p, n) Interaction

The proton production pathway for iron-55 is via Mn-55 (p, n) Fe-55 interaction. This reaction requires a minimum energy of 1.52 MeV (endothermic reaction), so ideally a surrogate would have a similar threshold energy for the production reaction. This pathway is present in all experiments, with deuterium and without. This surrogate pathway will be used in the non-deuterium surrogate correlation.

There is no detectable surrogate (by the established requirements) unique to the Mn-55 (p, n) Fe-55 production reaction with similar interaction energy and interaction probability. Due to this, a surrogate with (p, n) and (d, n) production mechanisms will be used. Cobalt-57 has a similar (p, n) Q value of -2.13 MeV and has nearly identical (p, n)

cross section. The surrogate is compared to the Mn-55 (p, n) Fe-55 production pathway in Table 6.

Table 6. Co-57 and Fe-55 by (p, n) interaction. National Nuclear Data Center. Nuclear Science References, (2007). Information extracted from the NSR database.

| Target | Reaction | Target Abundance (%) | Produced Radionuclide | Half Life | **Q (MeV)** |
|---|---|---|---|---|---|
| Fe-57 | p, n | 1.4 ± 0 | Co-57 | 312 d | **-2.13** |
| Mn-55 | p, n | < 2 | Fe-55 | 2.7 y | **-1.52** |

A comparison of their respective interaction probabilities is shown in Figure 4.

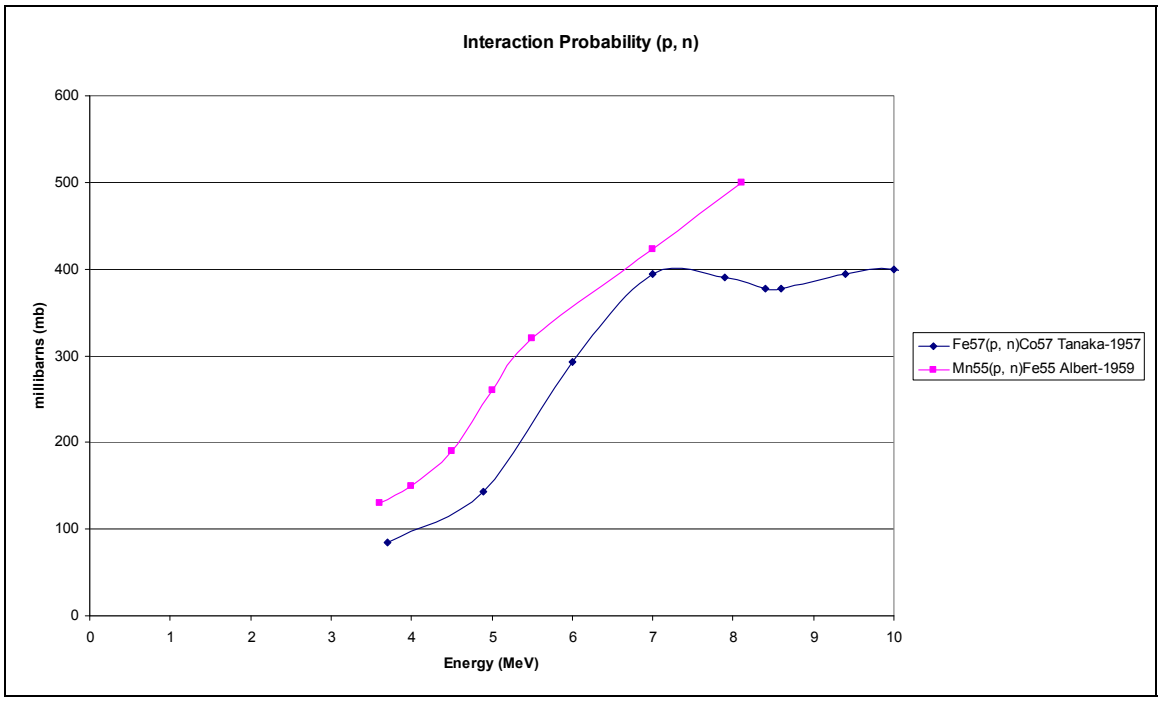


Fig. 4. Fe-57 (p, n) Co-57 and Mn-55 (p, n) Fe-55 probability vs. incident proton energy. Plot produced using the code JANIS, written by the OECD Nuclear Energy Agency and Aquitaine Electronique Informatique. OECD Nuclear Energy Agency. Le Seine Saint-Germain, France.

Due to the similarity of threshold energy and probability for reaction an interaction probability weighting factor $F_{(p,n)}^{Fe55}_{Co57}$ can be established. Cobalt-57

production from (d, n) interaction remains to be accounted. The use of cobalt-55 as this correction factor will be discussed in the correction factor subsection.

*Cobalt-57 Correction Factor*

Cobalt-57 is used as a surrogate for the (p, n) production mechanism surrogate but this requires exclusion of the contribution from (d, n) interaction. Cobalt-55, as used previously is primarily produced by (d, n) interaction (excluding the minimal (p, γ) contribution) and has similar (d, n) interaction probability to that of cobalt-57. The production characteristics of cobalt-55 and cobalt-57 by (d, n) interaction are shown in Table 7.

Table 7. Co-57 and Co-55 by (d, n) interaction. National Nuclear Data Center. Nuclear Science References, (2007). Information extracted from the NSR database.

| Target | Reaction | Target Abundance (%) | Produced Radionuclide | Half Life | Q (MeV) |
|---|---|---|---|---|---|
| Fe-54 | d, n | 4 ±0 | Co-55 | 17.5 | **2.83** |
| Fe-56 | d, n | 62.4 ± 0 | Co-57 | 271 d | **3.8** |

The Fe-54 (d, n) Co-55 and Fe-56 (d, n) Co-57 interaction probabilities are shown in Figure 5.

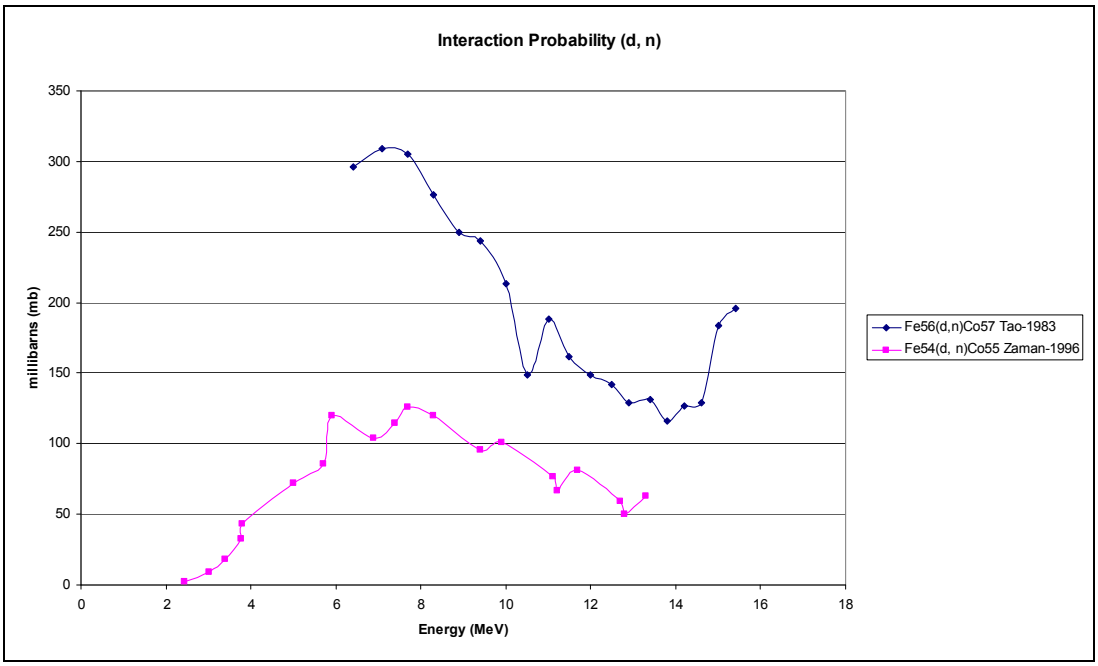


Fig. 5. Fe-54 (d, n) Co-55 and Fe-56 (d, n) Co-57 probability vs. incident deuteron energy. Plot produced using the code JANIS, written by the OECD Nuclear Energy Agency and Aquitaine Electronique Informatique. OECD Nuclear Energy Agency. Le Seine Saint-Germain, France.

Due to the similar (within a factor of 3.5) interaction probabilities, cobalt-55 can be used to determine cobalt-57 abundance from (d, n) interaction. Below 5.5 MeV (the deuteron energy range expected on the Z-machine) there seems to be a factor of 2-3 difference between the interaction probabilities. The interaction probability weighting will be notated $F_{(d,n)}^{Co57}{}_{Co55}$.

*Cobalt-57 Mathematical Correlation*

To account for (p, n) contribution to iron-55, total cobalt-57 activity must be corrected due to contribution from (d, n) production. As previously described, cobalt-55 can represent cobalt-57 production from (d, n) interaction, due to the similar interaction probability per atom. The following is the decay-corrected cobalt-57 abundance due to (p, n) interaction.

$$A_{o\,Co-57}^{p,n} = A_{0\,Co-57}^{total} - A_{o\,Co-57}^{d,n}$$

$$\frac{A_{o\,Co-57}^{d,n}}{A_{0\,Co-55}^{total}} = \frac{.624}{.04} * F_{(d,n)}^{Co57}{}_{Co55}$$

$$A_{o\,Co-57}^{p,n} = A_{0\,Co-57}^{total} - \frac{.624}{.04} * A_{0\,Co-55}^{total} * F_{(d,n)}^{Co57}{}_{Co55}$$

Where $A_0$ is the activity of the respective radionuclide at time = 0 and $\boldsymbol{F_{(d,n)}^{Co57}{}_{Co55}}$ is equal to the interaction probability weighting factor. $A_{o\,Co-57}^{p,n}$ activity is representative of iron-55 produced by (p, n) interaction. The decay corrected abundance of iron-55 from this mechanism is derived in Equation 4.

$$\frac{A_{0\,Fe-55}^{p,n}}{A_{o\,Co-57}^{p,n}} = \frac{.02}{.014} * F_{(p,n)}^{Fe55}{}_{Co57}$$

$$A_{0\,Fe-55}^{p,n} = \frac{.02}{.014} * A_{o\,Co-57}^{p,n} * F_{(p,n)}^{Fe55}{}_{Co57}$$

$$A(t)_{Fe-55}^{p,n} = A_{0\,Fe-55}^{p,n} * e^{(-\lambda_{Fe55}t)}$$

$$A(t)_{Fe-55}^{p,n} = \frac{.02}{.014} * F_{(p,n)}^{Fe55}{}_{Co57} * A_{o\,Co-57}^{p,n} * e^{(-\lambda_{Fe55}t)} \qquad (4)$$

Where $\boldsymbol{F_{(p,n)}^{Fe55}{}_{Co57}}$ is equal to the respective interaction probability weighting factor.

## 3.4 Total Correlation in Deuterium Loaded Interactions

Adding the activities derived for iron-55 from cobalt-55, cobalt-57 and chromium-51 gives the total estimated iron-55 activity in Equation 5:

$$A(t)^{total}_{Fe-55} = A(t)^{d,p;n,\gamma}_{Fe-55} + A(t)^{p,n}_{Fe-55} + A(t)^{Co\,55\rightarrow}_{Fe-55}$$

$$A(t)^{total}_{Fe-55} = [\frac{.04}{.008\pm0.0009} * F_{(d,\ p;\ n,\ \gamma)}{}^{Fe55}_{Cr51} * A^{d,p;n,\gamma}_{0Cr-51} * e^{(-\lambda_{Fe55}t)}] + \ldots$$

$$\ldots + [\frac{.02}{.014} * F_{(p,\ n)}{}^{Fe55}_{Co57} * A^{p,n}_{oCo-57} * e^{(-\lambda_{Fe55}t)}] + \ldots$$

$$\ldots + [\frac{A^{total}_{0Co-55}}{\lambda_{Co55}}(1 - e^{(-\lambda_{Co55}t)}) * e^{(-\lambda_{Fe55}t)} * \lambda_{Fe55}]$$

$$A(t)^{total}_{Fe-55} = [\frac{.04}{.008\pm0.0009} * F_{(d,\ p;\ n,\ \gamma)}{}^{Fe55}_{Cr51} * \{A^{total}_{0Cr-51} - \frac{.008\pm0.0009}{.04} * A^{total}_{0Co-55} * F_{(d,n)}{}^{Mn51}_{Co55}\} * e^{(-\lambda_{Fe55}t)}] +$$

$$\ldots + [\frac{.02}{.014} * F_{(p,\ n)}{}^{Fe55}_{Co57} * \{A^{total}_{0Co-57} - \frac{.624}{.04} * A^{total}_{0Co-55} * F_{(d,\ n)}{}^{Co57}_{Co55}\} * e^{(-\lambda_{Fe55}t)}] + \qquad (5)$$

$$\ldots + [\frac{A^{total}_{0Co-55}}{\lambda_{Co55}}(1 - e^{(-\lambda_{Co55}t)}) * e^{(-\lambda_{Fe55}t)} * \lambda_{Fe55}]$$

# 4. IRON-55 IN NON-DEUTERIUM LOADED REACTIONS

The absence of deuterium results in a much simpler correlation. Again, cobalt-55 decays directly to iron-55 and constitutes a contribution to total iron-55 abundance. The non-deuterium loaded production mechanisms of iron-55 are shown in Tables 8 and 9.

Table 8. Non-deuterium loaded direct production of iron-55. National Nuclear Data Center. Nuclear Science References, (2007). Information extracted from the NSR database.

| Target | Reaction | Target Abundance (%) | Produced Radionuclides | Half-Life | Q (MeV) |
|---|---|---|---|---|---|
| Fe-54 | n, γ | 4 ± 0 | Fe-55 | 2.7y | 9.3 |
| Mn-55 | p, n | < 2 | Fe-55 | 2.7y | -1.52 |

Table 9. Non-deuterium loaded indirect production of iron-55. National Nuclear Data Center. Nuclear Science References, (2007). Information extracted from the NSR database.

| Target | Reaction | Target Abundance (%) | Produced Radionuclides | Half-Life | Q (MeV) |
|---|---|---|---|---|---|
| Fe-54 | p, γ ** | 4 ± 0 | Co-55* | 17.5 h | 5.06 |

*Co-55 decays directly to Fe-55. ** Rare interaction

The reduction of pathways for iron-55 production relative to that of deuterium loaded interactions results in a simpler surrogate correlation. Analogous to deuterium loaded surrogates, a selection process was pursued on the radionuclides in Table 10 for possible use as a surrogate.

Table 10. Radionuclides from non-deuterium loaded interactions. National Nuclear Data Center. Nuclear Science References, (2007). Information extracted from the NSR database.

| **Target: 304 Stainless steel** Detected nuclide | Half-life | production reaction | Daughter | Daughter Half-life |
|---|---|---|---|---|
| Co-54 | 1.5m/193ms | p, n | Fe-54 | Stable |
| **Co-55** | **17.5 h** | **p, γ** | **Fe-55** | **2.73 yr** |
| Co-56 | 77.3d | p, n | Fe-56 | Stable |
| **Co-57** | **271d** | **p, n** | **Fe-57** | **Stable** |
| Mn-50 | 1.7m/283ms | p, n | Cr-50 | 1.8E+17 yr |
| Mn-52 | 21m/5.6d | p, n | Cr-52 | Stable |
| Mn-53 | 3.7x106y | p, n | Cr-53 | Stable |
| Mn-54 | 312 d | p, n | Cr-54 | Stable |
| Mn-56 | 2.6h | n, γ | Fe-56 | Stable |
| Cu-58 | 3.2s | p, n | Ni-58 | Stable |
| Cu-60 | 24ms | p, n | Ni-60 | Stable |
| Cu-61 | 3.4h | p, n | Ni-61 | Stable |
| Cu-62 | 9.7m | p, n | Ni-62 | Stable |
| Fe-55 | 2.73 y | p, n; n, γ | Mn-55 | Stable |
| **Cr-51** | **27d** | **n, γ** | **V-51** | **Stable** |
| Cr-55 | 3.5m | n, γ | Mn-55 | Stable |
| Ni-59 | 7.6x104y | n, γ | Co-59 | Stable |
| Ni-63 | 101y | n, γ | Cu-63 | Stable |

It can be observed in Table 10 that several radionuclide production pathways exist that are similar to iron-55 production pathways. Applying radiation type and half-life selection criteria to this list eliminates the majority of these. The total number of pathways is much lower than for deuterium loaded interactions. The surrogates selected remain the same as for deuterium loaded interactions: chromium-51, cobalt-55 and cobalt-57. However, the correction factors for chromium-51 and cobalt-57 are no longer required. Weighting factors relating the atomic abundances of the target materials, interaction probabilities and correcting for decay time discrepancy are implemented in the final mathematical expressions.

## 4.1 Cobalt-55 Decay

Unlike deuterium loaded interactions, cobalt-55 is rarely produced in non-deuterium shots via (p, γ) interaction. In one unique experimental session out of over 1000 there was an error in experimental setup that may have caused a higher than normal proton flux and cobalt-55 was detected. However, this is most likely not produced in the vast majority of experiments. Nevertheless, all cobalt-55 produced decays directly to iron-55 with a 17.5 hour half life. Therefore, all cobalt-55 that is detected must contribute to iron-55 abundance.

Co-55 decays directly to iron-55 with a 17.5 hr half life. The decay-corrected abundance of iron-55 from cobalt-55 decay as a function of time is derived in Equation 2.

## 4.2 Chromium-51 by (n, γ) Interaction

The Fe-54 (n, γ) Fe-55 production reaction is within an order of magnitude to the similar production interaction of Cr-50 (n, γ) Cr-51. In addition, chromium-51 is only produced directly by these reactions. This (n, γ) surrogate relation was used previously for deuterium loaded interactions but now has less contribution from interfering pathways. The direct production mechanisms are shown in Table 6. The respective interaction probabilities can be viewed in Figure 1. Due to these comparable interaction probabilities, the weighting factor $F_{(n,\gamma)}^{Fe55}{}_{Cr51}$ is established

*Chromium-51 Mathematical Correlation*

The decay corrected and atomically weighted abundance of iron-55 from (n, γ) interaction is shown in Equation 6.

$$\frac{A_{0\,Fe-55}^{n,\gamma}}{A_{0\,Cr-51}^{total}} = \frac{.04}{.008\pm0.0009} * F_{(n,\gamma)\,Cr\,51}^{Fe55}$$

$$A_{0\,Fe-55}^{n,\gamma} = \frac{.04}{.008\pm0.0009} * A_{0\,Cr-51}^{total} * F_{(n,\gamma)\,Cr\,51}^{Fe55}$$

$$A(t)_{Fe-55}^{n,\gamma} = A_{0\,Fe-55}^{n,\gamma} * e^{(-\lambda_{Fe55}t)}$$

$$A(t)_{Fe-55}^{n,\gamma} = \frac{.04}{.008\pm0.0009} * A_{0\,Cr-51}^{total} * F_{(n,\gamma)\,Cr\,51}^{Fe55} * e^{(-\lambda_{Fe55}t)} \quad (6)$$

Where $A_0$ is activity of the respective radionuclide at time = 0 and $\boldsymbol{F_{(n,\gamma)\,\mathbf{Cr\,51}}^{\mathbf{Fe55}}}$ is the respective interaction probability weighting factor.

## 4.3 Cobalt-57 by (p, n) Interaction

Similarly to the deuterium loaded experiments, the (p, n) pathway is Mn-55 (p, n) Fe-55 interaction (Q = -1.52 endothermic) and the chosen surrogate correlating to this production pathway is cobalt-57. However, deuterium interactions contributing to cobalt-57 are no longer existent. Therefore the correction factor to account for cobalt-57 from deuterium interaction is no longer needed. The cobalt-57 production pathway has a similar (p, n) Q value of -2.13 MeV and has a nearly identical (p, n) cross section seen in Table 6 and Figure 4. Due to these comparable interaction probabilities, the weighting factor $\boldsymbol{F_{(p,n)\,\mathbf{Co57}}^{\mathbf{Fe55}}}$ is established.

*Cobalt-57 Mathematical Correlation*

The decay corrected and atomically weighted abundance of iron-55 from (p, n) interaction is shown in Equation 7.

$$\frac{A_{0\,Fe-55}^{p,n}}{A_{o\,Co-57}^{total}} = \frac{.02}{.014} * F_{(p,n)_{Co57}}^{Fe55}$$

$$A_{0\,Fe-55}^{p,n} = \frac{.02}{.014} * A_{o\,Co-57}^{total} * F_{(p,n)_{Co57}}^{Fe55}$$

$$A(t)_{Fe-55}^{p,n} = A_{0\,Fe-55}^{p,n} * e^{(-\lambda_{Fe55}t)}$$

$$A(t)_{Fe-55}^{p,n} = \frac{.02}{.014} * F_{(p,n)_{Co\,57}}^{Fe\,55} * A_{o\,Co-57}^{total} * e^{(-\lambda_{Fe\,55}t)} \qquad (7)$$

Where $A_0$ is activity of the respective radionuclide at time = 0 and $F_{(p,n)_{Co57}}^{Fe55}$ is the respective interaction probability weighting factor.

## 4.4 Total Correlation in Non-Deuterium Loaded Interactions

Accounting for each iron-55 interaction pathway yields the following equation:

$$A(t)_{Fe-55}^{total} = A(t)_{Fe-55}^{n,\gamma} + A(t)_{Fe-55}^{p,n} + A(t)_{Fe-55}^{Co55\rightarrow}$$

Substituting the respective surrogate activities derived for iron-55 from cobalt-55, cobalt-57 and chromium-51 gives the total estimated iron-55 activity in Equation 8:

$$A(t)^{total}_{Fe-55} = [\frac{.04}{.008\pm0.0009} * A_{0\,Cr-51}^{total} * F_{(n,\gamma)\,Cr51}^{Fe55} * e^{(-\lambda_{Fe55}t)}] + \ldots$$
$$\ldots + [\frac{.02}{.014} * F_{(p,n)\,Co57}^{Fe55} * A_{o\,Co-57}^{total} * e^{(-\lambda_{Fe55}t)}] + \ldots \quad (8)$$
$$\ldots + [\frac{A_{0\,Co-55}^{total}}{\lambda_{Co55}}(1 - e^{(-\lambda_{Co55}t)}) * e^{(-\lambda_{Fe55}t)} * \lambda_{Fe55}]$$

Where $A_0$ is the activity of the respective radionuclide at time = 0 and the respective interaction probability weighting factors are $F_{(d,\,p;\,n,\,\gamma)\,Cr51}^{Fe55}$ and $F_{(p,\,n)\,Co57}^{Fe55}$.

# 5. SUMMARY AND CONCLUSIONS

The correlations shown between iron-55 and other more easily detected radionuclides have been derived by the preceding method for each type of Z-machine experiment, deuterium and non-deuterium. Weighting factors relating the atomic abundances of the target materials, interaction probability and correcting for decay time discrepancy are implemented in these final mathematical expressions.

## 5.1 Correlation to Iron-55 in Deuterium Loaded Interactions

If the ratio of proton flux to deuterium flux in deuterium interactions is on order of $10^3$ or higher, this relationship is deemed invalid. The probability of interaction for this proton absorption process is 3 orders of magnitude lower than competing processes. The neglected Fe-54 (p, $\gamma$) Co-55 interactions used for the cobalt-55 surrogate correlation then become substantial. This has only been observed when the standard experimental setup changes, increasing proton flux and energy as noted by the experimenter (Internal Memo).

Accounting for each iron-55 interaction pathway and substituting them for each selected radionuclide yields the total correlation to iron-55 abundance for deuterium loaded interactions in Equation 5. Should additional data be gathered, correction factors may be modified to improve estimation.

## 5.2 Correlation to Iron-55 in Non-Deuterium Loaded Interactions

The smaller amount of iron-55 production pathways relative to deuterium loaded interactions provides a simpler process for estimating iron-55 concentration. This correlation does not assume negligible proton flux, so the existence of substantial proton flux is unimportant for the validility of this correlation.

Similar to the deuterium surrogate correlation, accounting for each iron-55 interaction pathway and substituting them for each selected surrogate radionuclide yields the total correlation to iron-55 abundance. This correlation for non-deuterium loaded interactions is given in Equation 9. Should additional data be gathered, correction factors may be modified to improve estimation.

## 5.3 Conclusions

These final correlations are to be used as a basis for estimating the existence or non-existence of iron-55 for regulatory and disposal purposes following activation of 304 stainless steel used on the Z-machine accelerator.

The selection process resulted in chromium-51, cobalt-57 and cobalt-55 being chosen as optimal potential surrogates. Weighting factors relating to differences in atomic abundance, interaction probability and competing production pathways of the potential surrogates are presented. A decay corrected correlation of the surrogates (chromium-51, cobalt-57 and cobalt-55) to iron-55 for deuterium and non-deuterium loaded Z-machine driven reactions was derived.

The weighting factors presented here are estimates which are based on rough comparisons of cross-section graphs. Analysis considering factors such as energy spectrum criteria to provide refined weighting factors may be utilized in future work.

# REFERENCES

Culp, T. A. February 2007. Prediction of Accelerator-Produced Activation Products. Health Physics. Operational Radiation Safety. 92(2) Supplement 1:S57-S65

JANIS 3.0. (2007). [Computer Software]. OECD Nuclear Energy Agency. Le Seine Saint-Germain, France

# APPENDIX

Table A. Deuterium, neutron (d, n) reactions in 304 stainless steel. Culp, Todd. A Prediction of Accelerator-Produced Activation Products. Health Physics. Operational Radiation Safety. 92(2) Supplement 1:S57-S65, February 2007.

| Material | Percent of Mixture | Percent Natural Abundance | Weighted Percent Abundance | Error +/- | Reaction Product | Half-life | Q Value (MeV) |
|---|---|---|---|---|---|---|---|
| | | | | | | | |
| Iron | 68 | | | | | | |
| Fe-54 | +-0 | 5.9 | 4 | 0 | Co-55 | 17.5h | 2.83 |
| Fe-56 | | 91.8 | 62.4 | 0 | Co-57 | 271d | 3.8 |
| Fe-57 | | 2.1 | 1.4 | 0 | Co-58 | 9.1h/71d | 4.73 |
| | | | | | | | |
| Chromium | 18.75 | | | | | | |
| Cr-50 | +- 1.25 | 4.3 | 0.80625 | 0.09375 | Mn-51 | 46.2m | 3.08 |
| Cr-52 | | 83.8 | 15.7125 | 1.0875 | Mn-53 | $3.7x10^6$y | 4.34 |
| Cr-53 | | 9.5 | 1.78125 | 0.11875 | Mn-54 | 312d | 5.34 |
| Cr-54 | | 2.4 | 0.45 | 0.05 | Mn-55 | Stable | 5.84 |
| | | | | | | | |
| Nickel | 9.5 | | | | | | |
| Ni-58 | +- 1.5 | 68.3 | 6.4885 | 1.0245 | Cu-59 | 1.4m | 1.2 |
| Ni-60 | | 26.1 | 2.4795 | 0.3915 | Cu-61 | 3.4h | 2.58 |
| Ni-61 | | 1.1 | 0.1045 | 0.0165 | Cu-62 | 9.7m | 3.66 |
| Ni-62 | | 3.6 | 0.342 | 0.054 | Cu-63 | Stable | 3.9 |
| | | | | | | | |
| Manganese | < 2 | | | | | | |
| Mn-55 | | 100 | 2 | -2 | Fe-56 | Stable | 7.96 |

Table B: Deuterium, proton (d,p) reactions in 304 stainless steel. Culp, Todd. A Prediction of Accelerator Produced Activation Products. Health Physics. Operational Radiation Safety. 92(2) Supplement 1:S57-S65, February 2007.

| Material | Percent of Mixture | Percent Natural Abundance | Weighted Percent Abundance | Error +/- | Reaction Product | Half-life | Q Value (MeV) |
|---|---|---|---|---|---|---|---|
| | | | | | | | |
| Iron | 68 | | | | | | |
| Fe-54 | +-0 | 5.9 | 4 | 0 | Fe-55 | 2.7y | 7.58 |
| Fe-56 | | 91.8 | 62.4 | 0 | Fe-57 | stable | 5.93 |
| Fe-57 | | 2.1 | 1.4 | 0 | Fe-58 | stable | 8.33 |
| | | | | | | | |
| Chromium | 18.75 | | | | | | |
| Cr-50 | +- 1.25 | 4.3 | 0.80625 | 0.09375 | Cr-51 | 27d | 7.56 |
| Cr-52 | | 83.8 | 15.7125 | 1.0875 | Cr-53 | stable | 6.23 |
| Cr-53 | | 9.5 | 1.78125 | 0.11875 | Cr-54 | stable | 8.01 |
| Cr-54 | | 2.4 | 0.45 | 0.05 | Cr-55 | 3.5m | 4.54 |
| | | | | | | | |
| Nickel | 9.5 | | | | | | |
| Ni-58 | +- 1.5 | 68.3 | 6.4885 | 1.0245 | Ni-59 | $7.6 \times 10^4$y | 7.29 |
| Ni-60 | | 26.1 | 2.4795 | 0.3915 | Ni-61 | stable | 6.11 |
| Ni-61 | | 1.1 | 0.1045 | 0.0165 | Ni-62 | stable | 8.88 |
| Ni-62 | | 3.6 | 0.342 | 0.054 | Ni-63 | 101y | 5.15 |
| | | | | | | | |
| Manganese | < 2 | | | | | | |
| Mn-55 | | 100 | 2 | -2 | Mn-56 | 2.6h | 5.56 |

Table C. Neutron, gamma (n, γ) reactions in 304 stainless steel. Culp, Todd. A Prediction of Accelerator-Produced Activation Products. Health Physics. Operational Radiation Safety. 92(2) Supplement 1:S57-S65, February 2007.

| Material | Percent of Mixture | Percent Natural Abundance | Weighted Percent Abundance | Error +/- | Reaction Product | Half-life | Q Value (MeV) |
|---|---|---|---|---|---|---|---|
| | | | | | | | |
| Iron | | 68 | | | | | |
| Fe-54 | +-0 | 5.9 | 4 | 0 | Fe-55 | 2.7y | 9.3 |
| Fe-56 | | 91.8 | 62.4 | 0 | Fe-57 | stable | 7.64 |
| Fe-57 | | 2.1 | 1.4 | 0 | Fe-58 | stable | 10 |
| | | | | | | | |
| Chromium | 18.75 | | | | | | |
| Cr-50 | +- 1.25 | 4.3 | 0.80625 | 0.09375 | Cr-51 | 27d | 9.27 |
| Cr-52 | | 83.8 | 15.7125 | 1.0875 | Cr-53 | stable | 7.94 |
| Cr-53 | | 9.5 | 1.78125 | 0.11875 | Cr-54 | stable | 9.72 |
| Cr-54 | | 2.4 | 0.45 | 0.05 | Cr-55 | 3.5m | 6.25 |
| | | | | | | | |
| Nickel | 9.5 | | | | | | |
| Ni-58 | +- 1.5 | 68.3 | 6.4885 | 1.0245 | Ni-59 | $7.6 \times 10^4$y | 9 |
| Ni-60 | | 26.1 | 2.4795 | 0.3915 | Ni-61 | stable | 7.82 |
| Ni-61 | | 1.1 | 0.1045 | 0.0165 | Ni-62 | stable | 10.6 |
| Ni-62 | | 3.6 | 0.342 | 0.054 | Ni-63 | 101y | 6.86 |
| | | | | | | | |
| Manganese | < 2 | | | | | | |
| Mn-55 | | 100 | 2 | -2 | Fe-56 | stable | 7.96 |
| | | | | | | | |

Table D: Proton, neutron (p,n) reactions in 304 stainless steel. Culp, Todd. A Prediction of Accelerator-Produced Activation Products. Health Physics. Operational Radiation Safety. 92(2) Supplement 1:S57-S65, February 2007.

| Material | Percent of Mixture | Percent Natural Abundance | Weighted Percent Abundance | Error +/- | Reaction Product | Half-life | Q Value (MeV) |
|---|---|---|---|---|---|---|---|
| | | | | | | | |
| Iron | 68 | | | | | | |
| Fe-54 | +-0 | 5.9 | 4 | 0 | Co-54 | 1.5m | -9.54 |
| Fe-56 | | 91.8 | 62.4 | 0 | Co-56 | 77.3d | -5.87 |
| Fe-57 | | 2.1 | 1.4 | 0 | Co-57 | 271d | -2.13 |
| | | | | | | | |
| Chromium | 18.75 | | | | | | |
| Cr-50 | +- 1.25 | 4.3 | 0.80625 | 0.093 | Mn-50 | 1.7m | -8.89 |
| Cr-52 | | 83.8 | 15.7125 | 1.087 | Mn-52 | 21m/5.6d | -6 |
| Cr-53 | | 9.5 | 1.78125 | 0.118 | Mn-53 | 3.7e6y | -1.89 |
| Cr-54 | | 2.4 | 0.45 | 0.05 | Mn-54 | 312d | -2.67 |
| | | | | | | | |
| Nickel | 9.5 | | | | | | |
| Ni-58 | +- 1.5 | 68.3 | 6.4885 | 1.024 | Cu-58 | 3.2s | -9.86 |
| Ni-60 | | 26.1 | 2.4795 | 0.391 | Cu-60 | 24ms | -7.42 |
| Ni-61 | | 1.1 | 0.1045 | 0.016 | Cu-61 | 3.35h | -3.53 |
| Ni-62 | | 3.6 | 0.342 | 0.054 | Cu-62 | 9.74m | -5.23 |
| | | | | | | | |
| Manganese | < 2 | | | | | | |
| Mn-55 | | 100 | 2 | -2 | Fe-55 | 2.7y | -1.52 |
| | | | | | | | |

# VITA

Name: John Flores-McLaughlin

Address: Texas A&M University
Department of Nuclear Engineering
3133 TAMU
College Station, TX 77843

Email Address: johnfm@tamu.edu

Education: M.S., Health Physics, Texas A&M University, 2008
B.S., Nuclear Engineering, Texas A&M University, 2006